Ultrasonics - Sonochemistry 63 (2020) 104912

Contents lists available at ScienceDirect

Ultrasonics - Sonochemistry

journal homepage: www.elsevier.com/locate/ultson

Reaction kinetics of sonochemical oxidation of potassium hexacyanoferrate (II) in aqueous solutions

Paulina Rajchel-Mieldzioć[a], Ryszard Tymkiewicz[b], Jan Sołek[a], Wojciech Secomski[b], Jerzy Litniewski[b], Piotr Fita[a,*]

[a] Institute of Experimental Physics, Faculty of Physics, University of Warsaw, Pasteura 5, 02-093 Warsaw, Poland
[b] Institute of Fundamental Technological Research, Polish Academy of Sciences, Pawińskiego 5b, 02-106 Warsaw, Poland

ARTICLE INFO

Keywords:
Sonochemistry
Sonooxidation
Sonoreactor
Advanced oxidation processes
Waste-water treatment

ABSTRACT

We studied sonochemical reactions resulting from ultrasonic treatment of potassium hexacyanoferrate(II) in aqueous solutions using a custom-built apparatus working at 536 kHz. We concluded that primary reactions are completely dominated by oxidation of Fe(II) to Fe(III) and did not find any evidences for degradation of cyanide. At the highest concentration used in the present study (0.1 M) we detected formation of pentacyanoaquaferrate (II) complex, which is most probably formed in reactions between hexacyanoferrate(III) anions and hydrogen atoms or hydrated electrons formed in sonochemical processes. We also determined that hydroxyl radicals formation rate in our system, $(8.7 \pm 1.5)\cdot 10^{-8}$ M·s^{-1}, is relatively high compared to other reported experiments. We attribute this to focusing of the ultrasonic wave in the sample vessel. Finally, we suggest that oxidation rate of hexacyanoferrate(II) anions can be a convenient benchmark of efficiency of sonochemical reactors.

1. Introduction

The chemical effect of ultrasonically-induced or hydrodynamic cavitation has been long recognized as a potent tool for facilitating chemical reactions [1–9]. In particular, ultrasonic treatment of aqueous solutions leads to oxidation of dissolved substances and falls into the category of advanced oxidation process (AOP) [10–13]. The main process underlying oxidation in water exposed to ultrasound has been identified as generation of hydroxyl (OH·) radicals due to thermal dissociation of water in collapsing cavitation bubbles [11]. Reactions of these radicals with other molecules present in the solution may lead to formation of further oxidising species, especially if gases such as oxygen, nitrogen and ozone are dissolved. The catalogue of possible reactions occurring during sonochemical treatment of water is therefore very broad [14–16]. In addition to oxidation by OH· radicals, many reactions specific for dissolved chemicals can occur during ultrasonic treatment of aqueous solutions.

In recent years ultrasonic treatment gained popularity as a potential solution to the vital problem of purification of industrial wastewater [14,17,18]. Among other pollutants, cavitation-induced degradation has been demonstrated for cyanides [19–22]. The process was found to be especially effective when ultrasonic treatment was combined with UV irradiation and ozonation [21]. There is a great potential for its application in addition to traditional methods for cyanide removal [23] in order to reduce cost and increase efficiency of cyanide-containing wastewater treatment.

In the above mentioned works [20,21] potassium hexacyanoferrate (II) was used as a model contaminant and the rate of its degradation was interpreted as a measure of the efficiency of the ultrasonic treatment. Reactions occurring during its sonochemical decomposition have not been, however, studied so far. In principle, hexacyanoferrate(II) ions can participate in several chemical reactions potentially induced by ultrasonication. In particular, they can undergo chemical oxidation of Fe(II) by oxidising agents such as OH·, pyrolytic decomposition yielding free iron and cyanide ions, or oxidation of cyanide ions ultimately leading to their removal from the solution as gaseous products [21]. Hexacyanoferrate(II) ions are also known to undergo photooxidation by direct detachment of an electron [24–27] and photoaquation which is substitution of one of the cyanide groups with a water molecule after excitation with UV light of appropriate energy [28–31]. Extreme conditions in cavitation bubbles may also lead to electronic excitation of the ions, making both above processes possible under ultrasonic treatment. In order to shed light on the mechanism of ultrasonically induced decomposition of hexacyanoferrate(II) ions observed in the previous works, we decided to take a closer look on reactions occurring during sonochemical treatment of potassium

* Corresponding author.
E-mail address: fita@fuw.edu.pl (P. Fita).

https://doi.org/10.1016/j.ultsonch.2019.104912
Received 12 March 2019; Received in revised form 13 November 2019; Accepted 27 November 2019
Available online 30 November 2019

hexacyanoferrate(II) in aqueous solutions using optical absorption spectroscopy.

2. Material and methods

For exposition to ultrasound, 10 mL of potassium hexacyanoferrate (II) solution was placed in a cylindrical test tube made of fused silica. Internal and external diameters of the tube were equal to 1.5 and 2.0 cm, respectively. The solution was sonicated in a custom-built ultrasonic system that consisted of a flat, circular piezoelectric transducer (Pz26, 26 mm diameter, Meggitt, Kvistgaard, Denmark) located at the bottom of a water-filled cylinder made of polycarbonate (Fig. S1 in the Supporting Information; for convenience, the transducer arrangement with the cylindrical vessel is called the ultrasonic head in the article). The test tube with the solution was partially immersed in the cylinder, coaxially with the transducer axis.

The water in the cylinder served as a medium that transported ultrasound to the test tube and it was also a cooling medium. The cooling water was pumped continuously using a peristaltic pump through the polycarbonate cylinder and a cooling coil. Both the reservoir for the cooling water and the cooling coil were immersed in a laboratory bath chiller which maintained the appropriate temperature of the cooling liquid. This system allowed keeping a constant temperature of the sonicated solution even during a long-term ultrasonic exposure. The experiments were carried out with solutions kept at approximately room temperature (21 °C).

The transmission system for stimulating the piezoelectric transducer consisted of a signal generator (Rigol DG2041A) and a custom-built power amplifier (Institute of Fundamental Technological Research, Polish Academy of Sciences, Poland). Pulses with a length of 1000 cycles at 536 kHz and 135 V_{pp} amplitude were sent to the piezoelectric transducer with a repetition period of 3.72 ms (duty factor d_f = 0.5). The frequency of ultrasound used is almost optimal for the generation of hydroxyl radicals in argon-saturated water [32]. With these parameters, the average acoustic power emitted by the transducer, as measured by the radiation pressure balance (UPM-DT-1E, Ohmic Instruments, Easton, MD, USA), was P = 10 W.

Calorimetric measurements typically used to measure acoustic power delivered to the sonicated solution cannot be used in our setup due to the arrangement in which the cooling water is the ultrasound transmitting medium. Therefore power effectively transmitted to the sample was estimated on the basis of pressure measurements carried out using a 0.2 mm diameter needle hydrophone (Precision Acoustics, Dorchester, UK) calibrated at 536 kHz. Fig. 1 shows profiles of temporal-averaged ultrasonic intensity measured in the test tube containing 10 mL of water (66 mm above the transducer) and directly in the cylinder of the ultrasonic head filled with cooling water (the test tube was removed for the latter measurement).

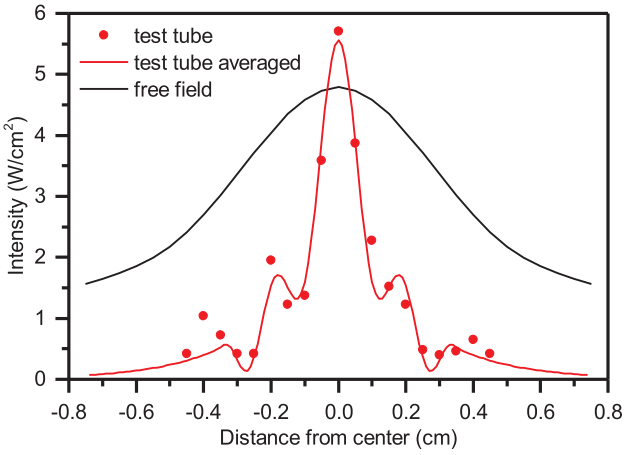

Fig. 1. Temporal-averaged ultrasound intensity profile measured along the diameter of the test tube and in free field (in the cylinder of the ultrasonic head) as well as averaged and interpolated values of intensity used for calculation of the power transmitted to the sample.

The maximum value of the spatial-peak, time-averaged ultrasonic intensity, measured in the sample tube centre was I_{SPTA} = 5.8 W/cm^2. The ultrasonic intensity during the pulse duration (spatial-peak pulse-average intensity) was twice as high and equal to $I_{SPPA} = I_{SPTA}/d_f$ = 11.6 W/cm^2 [33]. Due to focusing properties of the test tube and a number of additional acoustic effects resulting from the tube-ultrasound interaction the ultrasonic intensity in the test tube had a non-uniform distribution with a sharp peak in the centre. The maximum intensity measured in the centre of the test tube was actually higher than the value measured in free field (in the cylinder of the ultrasonic head) at the same transmitted ultrasound power. The average ultrasonic power inside the tube, calculated by integrating the I_{SPTA} distribution over the area of the test tube, was P_A = 0.64 W. Thus, the spatial-averaged, time averaged intensity inside the tube was I_{SATA} = 0.36 W/cm^2. It means that the peak intensity I_{SPPA} was more than 30 times higher than the average intensity. This fact might be very important for interpretation of the obtained results due to nonlinear nature of cavitation-induced processes, as it will be discussed later. The temporal-average energy density inside the tube was approx. ρ_{tube} = 0.064 W/cm^3. Summarized parameters of the sonication apparatus are collected in Table 1.

Studied solutions were prepared from potassium hexacyanoferrate (II) (Sigma-Aldrich) and potassium hexacyanoferrate(III) (Chempur) of analytical purity and water distilled in an all-glass distiller. For 15 min prior to experiments as well as during sonication the solutions were sparged with argon or air. Flow of the gas was kept between 10 and 30 mL/min.

Absorption spectra were measured with Perkin-Elmer Lambda 35 spectrophotometer in fused silica cuvettes with 10 mm optical path. If absorbance of sonicated solutions was too high to be measured with the spectrometer, they were diluted prior to absorption measurements. Otherwise their absorption was recorded and they were returned to the test tube for further sonication, if required.

3. Results

Fig. 2a shows UV/VIS absorption spectra of potassium hexacyanoferrate(II) solution in distilled water at the concentration of 0.0001 M during sonication at 536 kHz in presence of argon constantly flowing through the liquid. The initial spectrum is dominated by the strong absorption band of hexacyanoferrate(II) anions, centred at 218 nm [34]. During sonication this band diminishes, whereas characteristic bands of hexacyanoferrate(III) anions with maxima at approx. 260 nm, 303 nm and 420 nm arise [35]. After 60 min of sonication the 420 nm band practically overlaps with the corresponding band seen in the absorption spectrum of 0.0001 M potassium hexacyanoferrate(III) solution. Similar evolution of absorption spectra in the range of 250–470 nm is seen when the sonicated solution is sparged with air, however in this case the 420 nm band overlaps with the band of hexacyanoferrate(III) anion already after 20 min (Fig. 2b). Absorption of sonicated solutions at wavelengths shorter than 350 nm exceeds that of

Table 1
Parameters of the experimental setup used for sonication of studied solutions.

Sample volume	10 cm^3
Frequency	536 kHz
Burst length	1000 cycles
Burst period	3.72 ms
Average power transmitted to the sample P_A	≈0.64 W
Average intensity in the sample I_{SATA}	≈0.36 W/cm^2
Peak intensity in the sample I_{SPPA}	≈11.6 W/cm^2
Average energy density in the sample	≈ 0.064 W/cm^3

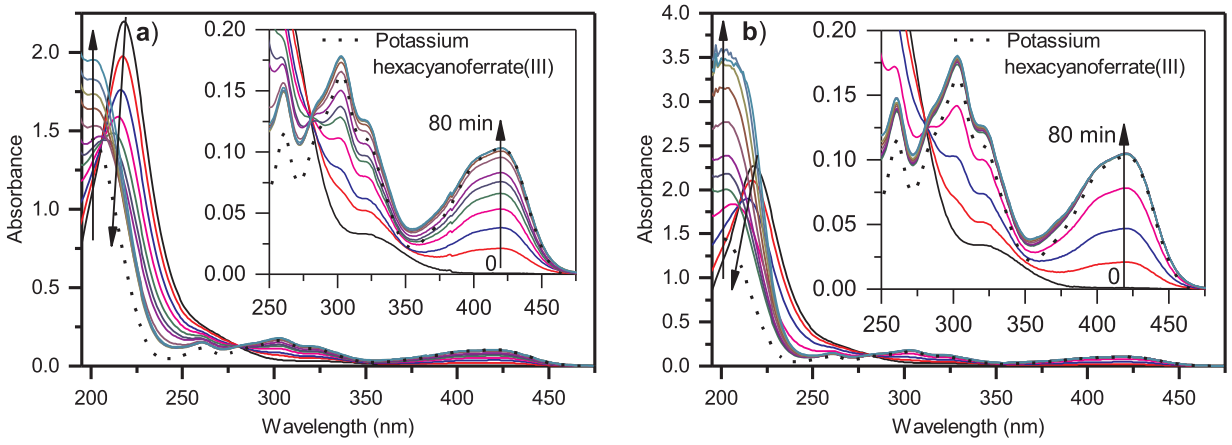

Fig. 2. Absorption spectra of 0.0001 M aqueous solution of potassium hexacyanoferrate(II) sparged with argon (a) and air (b) during sonication at 536 kHz. Solid lines correspond to sonication times: 0, 5, 10, 15, 20, 25, 30, 40, 50, 60, 70, 80 min. The dashed lines represent absorption spectrum of 0.0001 M solution of potassium hexacyanoferrate(III).

fresh hexacyanoferrate(III) solutions and a strong band centred at approx. 202 nm, absent in spectra of hexacyanoferrate(III) ions, appears. In spite of slightly different ultrasonic wave intensities in different experiments, the above described results can be very well reproduced in consecutive measurements as shown in Figs. S2 and S3 in the Supporting Information.

The 202 nm band grows significantly faster in air-saturated solutions and appears also during sonication of pure water (Fig. 3). Its position corresponds well to main UV absorption bands of NO_2^- and NO_3^- anions [36] which were detected in sonicated water [37–40]. Experiments carried out under carefully controlled conditions indicated that both oxygen and nitrogen must be dissolved in water for these ions to be formed [39,40]. Nevertheless, it was observed that they also appear in sonicated solutions purged with argon [38]. In the latter case oxygen and nitrogen are most probably introduced into the solution due to diffusion of air through the surface of the liquid when the solution is sonicated in a vessel open to ambient atmosphere. This also takes place in our experiments. The maximum of the observed absorption band is initially located at 205 nm for short sonication times and moves towards 200 nm. This observation agrees with the mechanism described in the literature, according to which NO_2^- anions, which absorb at longer wavelengths, predominate at early sonication times. They are gradually replaced by NO_3^- which have their absorption spectrum shifted towards shorter wavelengths with respect to NO_2^- [38,40].

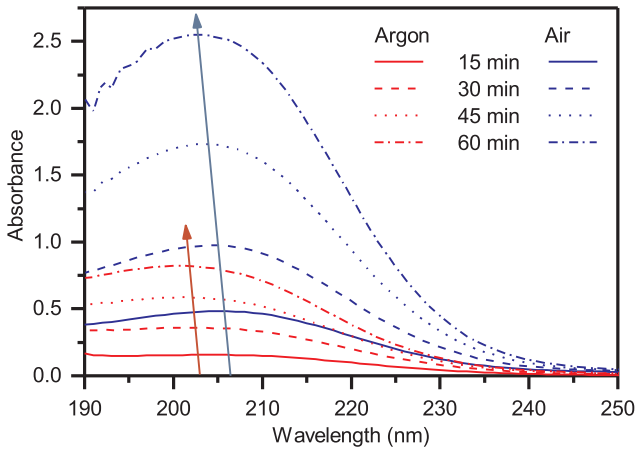

Fig. 3. Difference of absorption spectra of distilled water sonicated at 536 kHz for a given time and fresh distilled water used for preparing solutions. The sonicated sample was sparged with argon or air.

Hydrogen peroxide, efficiently formed during sonication of pure water, also absorbs in the spectral region below 300 nm but because of its very small extinction coefficient (dropping from 140 $M^{-1}cm^{-1}$ at 200 nm down to 1 $M^{-1}cm^{-1}$ at 300 nm) in comparison to nitrate (approx. 10^4 $M^{-1}cm^{-1}$ at 200 nm) and nitrite anions (approx. 5.5×10^3 $M^{-1}cm^{-1}$ at around 210 nm) [36] its contribution to absorption spectra of sonicated water in the range 200–300 nm is negligible.

Sonication of the hexacyanoferrate(II) solution at 0.0001 M in the above described conditions results in practically 100% oxidation of hexacyanoferrate(II) to hexacyanoferrate(III) anions within 60 min when the purging gas is argon. The time required for complete oxidation of the ions is shortened down to 20–30 min when the solutions is purged with air. Changes of the solution's absorbance at 420 nm during sonication are presented in Fig. 4. It can be safely assumed that sonochemical reactions of hexacyanoferrate(II) anions in the studied system are dominated by oxidation of Fe(II) to Fe(III) mainly by OH· radicals formed through sonolysis of water:

$$H_2O \rightarrow OH^{\cdot} + H^{\cdot} \quad \text{(I)}$$

$$OH^{\cdot} + Fe(CN)_6^{4-} \rightarrow Fe(CN)_6^{3-} + OH^- \quad \text{(II)}$$

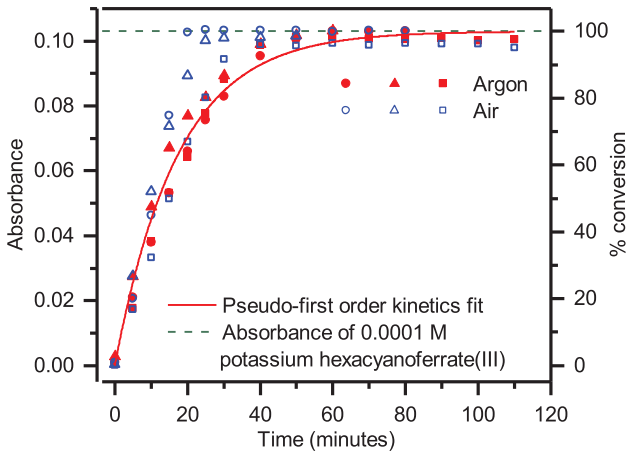

Fig. 4. Absorbance at 420 nm of 0.0001 M aqueous solution of potassium hexacyanoferrate(II) sparged with argon and air during sonication in three independent pairs of experiments (represented by circles, triangles and squares). The dashed line at $A = 0.103$ represents absorbance of 0.0001 M solution of potassium hexacyanoferrate(III).

The key role of OH· radicals in the observed reaction has been confirmed by sonication of 0.0001 M deoxygenated solution of hexacyanoferrate(II) in presence of a hydroxyl radicals scavenger, namely 2-propanol at 0.05 M (Fig. S4 in the Supporting Information). Because in this case oxidation of hexacyanoferrate(II) anions competes with reaction of hydroxyl radicals with the alcohol, the hexacyanoferrate(II) oxidation is hindered to the extent that reflects the excess of alcohol and the ratio of second order reaction rate constants for reactions of OH · radicals with hexacyanoferrate(II) and 2-propanol, equal to approx. 10^{10} $M^{-1}s^{-1}$ and $2{\cdot}10^{9}$ $M^{-1}s^{-1}$, respectively[41].

What is important, no reactions leading to permanent decomposition of the complex are observed. The final concentration of hexacyanoferrate(III) anions is, within the accuracy of our experiments, equal to the initial concentration of potassium hexacyanoferrate(II).

The kinetic data for argon-saturated solutions, collected in three independent experiments, can be very well fitted with a single pseudo-first order kinetics (Fig. 4). Thus, one can attempt to analyse the kinetic data in a steady-state approximation, assuming that the concentration of hydroxyl radicals is approximately constant during the time of the experiment. The rate equation for oxidation of hexacyanoferrate(II) anions is

$$\frac{d[Fe(CN)_6^{4-}]}{dt} = -k_{ox}[OH^{\cdot}][Fe(CN)_6^{4-}] \quad (1)$$

where k_{ox} is the second order reaction rate, equal to approx. $k_{ox} = 1.05{\cdot}10^{10}$ $M^{-1}s^{-1}$ [41,42]. For a constant concentration of hydroxyl radicals, [OH·] ≈ const., the solution of this equation gives the pseudo-first order reaction kinetics for the concentration of hexacyanoferrate(II) anions:

$$[Fe(CN)_6^{4-}] = C_0 e^{-k_{ox}[OH^{\cdot}]t} = C_0 e^{-k't} \quad (2)$$

where C_0 is the initial concentration of hexacyanoferrate(II) anions and $k' = k_{ox}$[OH·] has the meaning of the pseudo-first order rate constant (for a given C_0) of oxidation of these anions. No decomposition of the complex is observed, thus the concentration of oxidised anions can be expressed as:

$$[Fe(CN)_6^{3-}] = C_o - [Fe(CN)_6^{4-}] = C_0(1 - e^{-k't}) \quad (3)$$

Absorbance of the solution at 420 nm can be described by the formula:

$$A_{420}(t) = d\varepsilon_{420}[Fe(CN)_6^{3-}] = d\varepsilon_{420}C_0(1 - e^{-k't}) \quad (4)$$

where $d = 1$ cm is the thickness of the cuvette used for absorption measurements and ε_{420} is the molar extinction coefficient of hexacyanoferrate(III) anions at 420 nm, equal to $\varepsilon_{420} = 1030$ $M^{-1}cm^{-1}$. Function (4) was fitted to the experimental data shown in Fig. 4, yielding $k' = (9.6 \pm 0.3){\cdot}10^{-4}$ s^{-1} for the merged data from three experiments carried out at $C_0 = 0.0001$ M. The concentration of OH· radicals under these conditions can be estimated as [OH·] ≈ $9{\cdot}10^{-14}$ M.

In the pseudo-steady state approximation the concentration of OH· radicals is given by the equilibrium between their formation in cavitation bubbles and their scavenging in reactions with other species present in the solution. Thus, the higher the concentration of hexacyanoferrate(II) anions is, the lower OH· concentration and $k' = k_{ox}$[OH·] are. The kinetic equation for the concentration of OH· radicals can be written as

$$\frac{d[OH^{\cdot}]}{dt} = f - k_{ox}[OH^{\cdot}][Fe(CN)_6^{4-}] - k_s[OH^{\cdot}] \quad (5)$$

where f is the formation rate of OH·. k_s describes all other reactions leading to scavenging of OH· radicals in the pseudo-first order approximation for these reactions (we neglect formation of hydrogen peroxide in OH· + OH· reaction due to low concentration of these radicals in the solution of hexacyanoferrate(II)). In the pseudo-steady state, for a short period of time when concentrations of all involved reactants can be considered to be constant,

$$f - k_{ox}[OH^{\cdot}][Fe(CN)_6^{4-}] - k_s[OH^{\cdot}] = 0 \quad (6)$$

Eq. (6) shows that the concentration of OH· radicals can be approximately constant during oxidation of hexacyanoferrate(II) only if $[Fe(CN)_6^{4-}] \approx const.$, i.e. for reaction times much shorter than the time needed to oxidise all hexacyanoferrate(II) ions present in the solution. For such short reaction times the exponential function $e^{-k't}$ can be approximated by $1 - k't$. The pseudo-first order kinetics (3) becomes then:

$$[Fe(CN)_6^{3-}] = C_o k't \quad (7)$$

Eq. (7) allows determination of k' for a given initial concentration of hexacyanoferrate(II) anions C_0 if only the initial part of the experimental kinetics is fitted. Experimental values of $[Fe(CN)_6^{3-}]$ were determined by measurements of the absorbance of the solution at 420 nm (solutions with initial hexacyanoferrate(II) concentration of 0.001 M and 0.1 M were diluted to 0.0001 M prior to absorption measurements and the resulting concentration was scaled appropriately). Initial values of k' were determined by fitting function (7) to the approximately linear part of the dependence of concentration of hexacyanoferrate(III) anions on the sonication time for argon-saturated solutions (Fig. 5a). Next, oxidation efficiencies, expressed in terms of moles of oxidised ions per unit energy were calculated using fitted values of k':

$$\eta = \frac{C_0 k' V}{P_A} \quad (8)$$

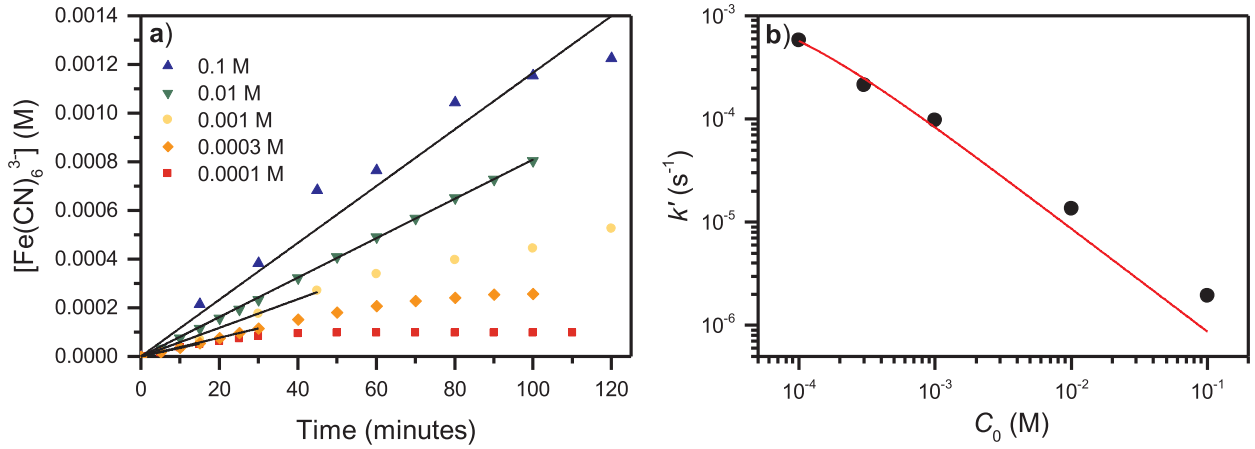

Fig. 5. a) Temporal dependence of hexacyanoferrate(III) anions concentration for different initial concentrations of potassium hexacyanoferrate(II). b) Dependence of initial values of k' on the initial concentration C_0 of potassium hexacyanoferrate(II).

Table 2
Initial reaction rates of hexacyanoferrate(II) oxidation (C_0k'), calculated initial values of k' used for determination of the hydroxyl radical formation rate and oxidation efficiencies η.

C_0 (M)	C_0k' ($M{\cdot}s^{-1}$)	k' (s^{-1})	η ($mol{\cdot}J^{-1}$)
0.0001	$(5.8 \pm 0.1){\cdot}10^{-8}$	$(5.8 \pm 0.1){\cdot}10^{-4}$	$9.1{\cdot}10^{-10}$
0.0003	$(6.40 \pm 0.04){\cdot}10^{-8}$	$(2.13 \pm 0.02){\cdot}10^{-4}$	$1.0{\cdot}10^{-9}$
0.001	$(9.8 \pm 0.4){\cdot}10^{-8}$	$(9.8 \pm 0.4){\cdot}10^{-5}$	$1.5{\cdot}10^{-9}$
0.01	$(1.35 \pm 0.05){\cdot}10^{-7}$	$(1.35 \pm 0.05){\cdot}10^{-5}$	$2.1{\cdot}10^{-9}$
0.1	$(1.95 \pm 0.10){\cdot}10^{-7}$	$(1.95 \pm 0.10){\cdot}10^{-6}$	$3.0{\cdot}10^{-9}$

Values of C_0k', k' and η for various concentrations are collected in Table 2.

Substitution of $k_{ox}[OH\cdot] = k'$ and $[Fe(CN)_6^{4-}] = C_0$ into Eq. (6) results in the formula (9) that describes the dependence of the initial oxidation rate on the initial concentration of hexacyanoferrate(II) anions C_0:

$$k'(C_0) = \frac{f}{C_0 + \frac{k_s}{k_{ox}}} \tag{9}$$

Fitting of function (9) to the initial values of k' measured for various C_0 (Fig. 5 b) allows determination of the formation rate f of hydroxyl radicals. The following values of parameters were found:

$f = (8.7 \pm 1.5){\cdot}10^{-8}\,M{\cdot}s^{-1}$

$k_s = (5.5 \pm 3.0){\cdot}10^{5}\,s^{-1}$

The above calculations were based on the pseudo-steady state approximation and a very simple model described by Eqs. (1) and (5). We decided to verify, how well this model describes the experimental data beyond the steady-state approximation. For this reason we numerically solved the set of differential Eqs. (1) and (5) with the above values of parameters f and k_s using Wolfram Mathematica software. Comparison of numerical solutions with experimental kinetics is shown in Fig. S5a in the Supporting Information. It can be seen that whereas the numerical solutions quite well describe the data for lower concentrations, the calculated kinetics are slower than experimental ones for the two highest concentrations (which can be also seen in Fig. 5b). This probably means that for high hexacyanoferrate(II) concentrations the concentration of hydroxyl radicals is low enough for another oxidation mechanism to become significant. It may be a reaction with hydrogen peroxide or other oxidative species formed in cavitation bubbles. Agreement of calculated kinetics with experimental data can be improved if a term of the form $-k_x[Fe(CN)_6^{4-}]$ which describes this additional oxidation channel is added to the right-hand side of Eq. (1). Comparison of oxidation kinetics calculated for $k_x = 1.5{\cdot}10^{-6}\,s^{-1}$ with experimental data is shown in Fig. S5b.

The kinetics obtained for the 0.0001 M solution sparged with air clearly deviate from the pseudo-first order kinetics (Fig. 4, blue data points). However, during the first 5 min of sonication the reaction rates are identical with both purging gases. Pairs of data points obtained for argon- and air-saturated solutions in each of the 3 repetitions of the experiment overlap each other after 5 min, in spite of certain differences between different repetitions. This fact is in excellent agreement with calculations of Merouani *et al.*, who predicted nearly identical rates of OH· radicals formation for sonication of air- and argon-saturated water at frequencies around 500 kHz [32]. At later times the concentration of oxidised anions in air-saturated solution becomes higher than described by the pseudo-first order kinetics. This means that the apparent reaction rate increases with sonication time. We attribute this increase of the oxidation rate of hexacyanoferrate(II) to production of H_2O_2 in combination with nitrate and nitrite anions during sonication of air-saturated water. Formation of nitrate and nitrite anions leads to the decrease of pH. Then, reactions of hexacyanoferrate(II) anions with hydrogen peroxide and nitrate anions in acidic solution become additional oxidation channels when concentration of these sonochemical products increases.

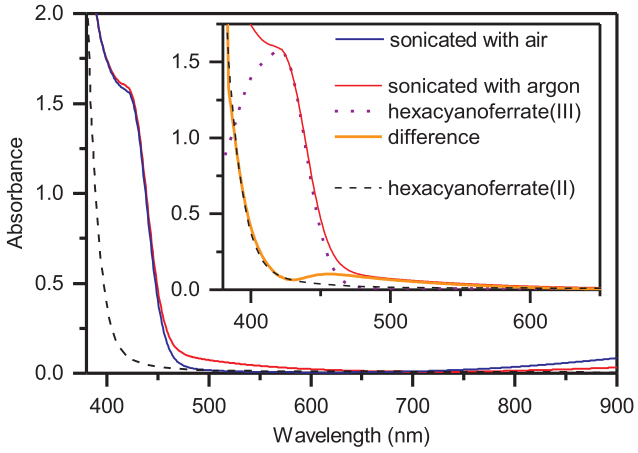

Fig. 6. Absorption spectra of 0.1 M solutions of potassium hexacyanoferrate(II) in air- and argon-saturated water sonicated for 120 min. The "difference" curve in the inset shows the difference between the spectrum of the argon-saturated solution and spectrum of potassium hexacyanoferrate(III) solution with concentration corresponding to the concentration of hexacyanoferrate(III) anions in the sonicated solution.

In order to look for other potential low-yield products of sonochemical reactions in the studied system we looked carefully at the absorption spectra of solutions sonicated for 120 min at the hexacyanoferrate(II) concentration of 0.1 M (Fig. 6). In particular, if cyanide anions were decomposed, the stoichiometry of the hexacyanoferrate complex would be disturbed and free iron cations released. Presence of free Fe(II) or Fe(III) would lead to appearance of the Prussian Blue complex which absorbs light in the red part of the absorption spectrum. Nevertheless, we cannot see any absorption band that could be attributed to Prussian Blue which has the absorption maximum at approx. 750 nm [43]. The lack of Prussian Blue in the sonicated solution means that no free iron cations are released from hexacyanoferrate complexes. This observation is another confirmation that under experimental conditions of the current study no optically detectable fraction of cyanide anions is decomposed and released from the solution as a direct result of ultrasonic treatment. Sensitivity of the Prussian Blue method was confirmed by appearance of blue colour in sonicated solutions stored for a couple of days. In this case hexacyanoferrate complexes are slowly decomposed due to the presence of nitric acid in the solution.

Additionally, we tried to directly detect potential products of cyanide oxidation, CO_2 and acetic acid, that should be produced in detectable quantities if a significant fraction of cyanide was oxidised. For this reason a 0.1 M solution of potassium hexacyanoferrate(II) sonicated for 60 min was analysed with methods of qualitative analysis (details and estimation of their sensitivity are given in the Supporting Information). The outflow of gas from the sonicated solution sparged with argon passed through a saturated solution of calcium hydroxide. Absorbance of the latter was examined at ten-minute intervals. No changes in transparency of the solution were observed, which indicates no detectable amount of carbon dioxide in the gaseous reaction products (the result of the test would be positive if more than 0.43% of carbon content was transferred to the test solution in the form of CO_2). A qualitative analysis of the sonicated solution for the acetate content was carried out by looking for the possible formation of a blue iodine complex on the surface of lanthanum hydroxyacetate. No acetates were detected within the sensitivity limit of the method, which was determined to be 0.00875 M.

In the absorption spectrum of the argon-saturated solution we can see a small increase of the absorption in the range 450–600 nm (Fig. 6).

Absorption of the sonicated solution in this spectral range exceeds the absorption of pure potassium hexacyanoferrate(III) solution scaled to a concentration corresponding to concentration of hexacyanoferrate(III) anions in the sonicated sample (inset in Fig. 6). Difference of the absorption spectrum of the sonicated solution and potassium hexacyanoferrate(III) solution reveals an absorption band centred at 450 nm. Position of this band corresponds to the absorption spectrum of the aquated $Fe(CN)_5H_2O^{3-}$ complex [29]. Extinction coefficient of the aquated complex at the absorption maximum is equal to 650 M^{-1} cm^{-1} [31], which allows for estimation of its concentration to $1.5{\cdot}10^{-4}$ M, approximately 10 times lower than concentration of $Fe(CN)_6^{3-}$ in the solution sonicated for 120 min. This complex is produced during illumination of hexacyanoferrate(II) solutions with ultraviolet light corresponding to the weak "shoulder" absorption band extending between 320 and 400 nm [26,28,29,31]. In principle one could think of its formation due to absorption of sonoluminescence light. However, generation of the aquated complex at the observed concentration in 10 mL solution would require absorption of approx. 10^{18} photons at the photoaquation yield of 0.9 [29]. This corresponds to the total energy of absorbed photons close to 0.5 J, which would require the power of the sonoluminescence light emitted in the UV range of the order of 10^{-5}–10^{-4} W which is unreasonably high for multibubble sonoluminescence.

The most probable mechanism of the aquated complex formation involves a reaction between $Fe(CN)_6^{3-}$ and hydrogen atoms formed through sonolysis of water [44]:

$$H^{\cdot} + Fe(CN)_6^{3-} \xrightarrow{H_2O} Fe(CN)_5H_2O^{3-} + HCN \quad \text{(III)}$$

Another reaction may involve hydrated electrons [44]:

$$e_{aq}^{-} + Fe(CN)_6^{3-} \xrightarrow{H_2O} Fe(CN)_5H_2O^{3-} + CN^{-} \quad \text{(IV)}$$

Even though formation of hydrated electrons during sonication of neutral water was questioned [45], it was shown that they are generated during sonication of argon-saturated solutions at multi 100-kHz frequency [46]. The fact that the $Fe(CN)_5H_2O^{3-}$ complex is formed from hexacyanoferrate(III) and not directly from hexacyanoferrate(II) anions explains why the aquated complex is not observed during sonication of 0.0001 M hexacyanoferrate(II) solutions. In this case the final concentration of $Fe(CN)_6^{3-}$ is more than an order of magnitude lower than its concentration after 120 min sonication of 0.1 M solution of potassium hexacyanoferrate(II). Consequently, the aquated complex is formed at such a low concentration that it is optically undetectable. On the other hand, the lack of the band attributed to the aquated complex in absorption spectra of the air-saturated solution may be explained by lower temperatures reached in cavitation bubbles and much lower generation yield of atomic hydrogen in sonicated air-saturated water compared to argon-saturated water [32].

4. Discussion

A striking observation emerging from the current study is the lack of any evidence of sonochemical decomposition of cyanide anions. This is in clear contrast to results described in the literature. During experiments presented in Refs. [20] and [21] degradation of up to 20% of cyanide was seen in 80–90 min, even for initially neutral solutions. This difference can be probably attributed to significantly different experimental conditions. At high ultrasound frequency used in our work the primary sonochemical process is generation of OH· radicals which act as very strong oxidative agents on dissolved chemicals, including free cyanide. However, in case of hexacyanoferrate(II) solutions all cyanide is bound in the very stable complex with Fe(II). Fe(II) in this complex is very easily oxidised, therefore the reaction of a hydroxyl radical with the complex leads to the detachment of an electron from iron and scavenging of the radical. On the other hand, oxidation of free cyanide groups by hydroxyl radicals first leads to formation of cyanate anions CNO^{-} [47]. In the case of a cyanide anion complexed with iron this would require detachment of the anion from the complex, energetically very unfavourable process. The latter fact also explains why cyanide in already oxidised hexacyanoferrate(III) complexes does not udergo easy oxidation by OH·, either.

At low frequency of ultrasound (22 and 25 kHz) used in the above-referenced works both temperature reached inside cavitation bubbles in water [48] and the cavitation threshold [49] are lower than at hundreds kHz. At the same time, high energy densities are used in low-frequency sonochemical reactors: in case of Ref. [20], the energy density, up to 0.75 W/cm^3, was more than 10 times higher than that used in our work. These factors together result in higher density of "hot spots" which are colder than those formed at high frequencies and low powers. The hydroxyl radicals formation rate decreases as a result of lowered temperature, but larger number of bubbles favours pyrolytic decomposition of the hexacyanoferrate complex, which does not require as high temperatures for decomposition as water: in vacuum hexacyanoferrates decompose at temperatures exceeding approx. 700 K whereas thousands K are needed for efficient decomposition of water. Therefore in high-power low-frequency sonoreactors, a significant fraction of cyanide is probably pyrolytically released from hexacyanoferrate complexes and can react with hydroxyl radicals before forming the complex with iron again.

The above explanation is fully consistent with experiments in which potassium cyanide and potassium hexacyanoferrate(II) were treated with the Fenton's reagent (1% H_2O_2 and 10 mM $FeSO_4$) which chemically generates hydroxyl radicals [50]. Cyanide was efficiently oxidised in spite of presence of iron in the reaction mixture, in contrast to hexacyanoferrate(II) complex which was oxidised with much lower yields. This result proves that free cyanide can be oxidised by hydroxyl radicals before it forms the complex with iron. However, after the hexacyanoferrate complex is formed, cyanide becomes resistant to oxidation by OH· radicals.

The methodology presented in this work allowed for fairly accurate determination of the formation rate of hydroxyl radicals f. Their scavenging rate k_s is determined with relatively low accuracy, but within the experimental error limits it is equal to the predicted value ($2.2{\cdot}10^5$ s^{-1} for a neutral solution [51]). Direct comparison of f with other experiments is difficult due to very large differences between conditions of sonochemical experiments carried out in various laboratories. One of works carried out under comparable conditions is reported in Ref. [52]: hydroxyl radicals generation rate was measured for sonication at 513 kHz with ultrasound intensity of 1.5 W/cm^2 and energy density 0.065 W/cm^3. Formation rate of OH· radicals was determined to be $6{\cdot}10^{-9}$ M/s, which is an order of magnitude less than in our experiments. For comparison of rates obtained under different conditions the Authors of Ref. [52] propose normalization according to the formula:

$$f_{norm} = f_{obs}\left(\frac{I_{ref}}{I}\right)\left(\frac{\rho_{ref}}{\rho}\right) \quad (10)$$

where f_{obs} is the rate measured at the wave intensity I and energy density ρ. f_{norm} is the rate scaled to reference intensity I_{ref} and reference energy density ρ_{ref}. If we normalize the value from Ref. [52] using the average ultrasound intensity in our apparatus we obtain an even lower value of f_{norm}. However, if we take the peak intensity value in our setup I_{SPPA} = 11.6 W/cm^2 as I_{ref}, we obtain the normalized hydroxyl generation rate $f_{norm} = 4.3{\cdot}10^{-8}$ M/s, closer to the value determined in our experiments. Thus, it seems that it is rather the peak ultrasound intensity and not its average value that determines the sonochemical efficiency.

Oxidation efficiencies, expressed in moles of the oxidised product per energy unit delivered to the sample, can be compared with values given in Refs. [53] and [54]. In these works sonochemical oxidation of potassium iodide was studied at various ultrasound frequencies. The

comparison is justified because reaction rates for oxidation of potassium iodide and potassium hexacyanoferrate(II) by hydroxyl radicals are nearly the same [41]. In Ref. [19] oxidation rate at 62 kHz, 6 W for initial concentration of KI equal to 0.1 M was reported to be $1.7{\cdot}10^{-10}$ mol/J. This number is almost 20 times lower than the oxidation efficiency of hexacyanoferrate(II) at the same initial concentration determined in our apparatus (approx. $3{\cdot}10^{-9}$ mol/J). Such a vast difference can be partially explained by significantly lower OH· formation rates at 62 kHz compared to 536 kHz, however the high peak intensity in our setup undoubtedly also plays a role here.

In Ref. [54] oxidation efficiencies of potassium iodide were studied for a concentration of 3.5% wt. (approx. 0.2 M) in sonochemical reactors working at 640 kHz with 258 W (0.75 L sample volume) and 396 W (0.6 L) transducers. Efficiency values between $0.68{\cdot}10^{-9}$ mol/J and $1.3{\cdot}10^{-9}$ mol/J were reported. These values are closer to oxidation rates in our setup, however still significantly lower. Considering the presented results, the hydroxyl radical generation rate and consequently oxidation efficiencies in our apparatus are relatively high. We attribute this fact to the focusing effect of the test tube, which results in very high ultrasound intensity in the centre of the sample. Our experiments suggest that using focused ultrasound beams in sonochemical reactors should significantly improve their efficiency without the need to increase the average power and total energy delivered to the sample.

5. Conclusions

We studied sonochemical reactions resulting from exposition of potassium hexacyanoferrate(II) solutions to ultrasonic waves at the frequency of 536 kHz in a custom-built apparatus. At the sonication frequency used in our study the primary reaction is predominated by oxidation of Fe(II) to Fe(III) in both argon- and air-saturated solutions. Analysis of oxidation kinetic rates allowed determination of hydroxyl radicals formation rate, which turned out to be significantly higher than values reported for other experiments carried out at comparable conditions. We attribute this fact to the focusing effect of the test tube used in our setup.

We cannot see any evidence for degradation of cyanide or other reactions of the hexacyanoferrate(II) complex under the conditions used in this study. Only, at the highest studied concentration of the potassium hexacyanoferrate(II) we presumably detected formation of the pentacyanoaquaferrate(II) complex in a reaction between hexacyanoferrate(III) anions and sonochemically formed hydrogen atoms or hydrated electrons.

Finally, we suggest that oxidation of the hexacyanoferrate(II) complex can be a convenient benchmark for efficiency of sonochemical reactors. This complex has a high reaction rate of oxidation by hydroxyl radicals and in contrast to potassium iodide commonly used for this purpose, the oxidation product of hexacyanoferrate(II) absorbs light in the blue part of the visible spectrum. It allows absorption measurements with blue LED or 405 nm laser diodes and a basic photodiode detector. Such a simple device could be used for absorption measurements *in situ*, in sonochemical reactors.

Declaration of Competing Interest

The authors declare that they have no known competing financial interests or personal relationships that could have appeared to influence the work reported in this paper.

Acknowledgements

This work was supported by National Science Centre, Poland, through project 2018/02/X/ST4/02439. The authors thank Piotr Hanczyc for proof-reading the manuscript.

Appendix A. Supplementary data

Supplementary data to this article can be found online at https://doi.org/10.1016/j.ultsonch.2019.104912.

References

[1] K.S. Suslick, Sonochemistry, Science 247 (1990) 1439–1445.
[2] K.S. Suslick, S.J. Doktycz, E.B. Flint, On the origin of sonoluminescence and sonochemistry, Ultrasonics 28 (1990) 280–290, https://doi.org/10.1016/0041-624X(90)90033-K.
[3] T.J. Mason, J.P. Lorimer, Sonochemistry: Theory, Applications and Uses of Ultrasound in Chemistry, Prentice Hall, New Jersey, 1989.
[4] R.J. Wood, J. Lee, M.J. Bussemaker, A parametric review of sonochemistry: Control and augmentation of sonochemical activity in aqueous solutions, Ultrason. Sonochem. 38 (2017) 351–370, https://doi.org/10.1016/j.ultsonch.2017.03.030.
[5] N. Pokhrel, P.K. Vabbina, N. Pala, Sonochemistry: Science and Engineering, Ultrason. Sonochem. 29 (2016) 104–128, https://doi.org/10.1016/j.ultsonch.2015.07.023.
[6] P. Cintas, S. Tagliapietra, M. Caporaso, S. Tabasso, G. Cravotto, Enabling technologies built on a sonochemical platform: challenges and opportunities, Ultrason. Sonochem. 25 (2015) 8–16, https://doi.org/10.1016/j.ultsonch.2014.12.004.
[7] R. Patil, P. Bhoir, P. Deshpande, T. Wattamwar, M. Shirude, P. Chaskar, Relevance of sonochemistry or ultrasound (US) as a proficient means for the synthesis of fused heterocycles, Ultrason. Sonochem. 20 (2013) 1327–1336, https://doi.org/10.1016/j.ultsonch.2013.04.002.
[8] B. Banerjee, Recent developments on ultrasound assisted catalyst-free organic synthesis, Ultrason. Sonochem. 35 (2017) 1–14, https://doi.org/10.1016/j.ultsonch.2016.09.023.
[9] K.S. Suslick, M.M. Mdleleni, J.T. Ries, Chemistry induced by hydrodynamic cavitation, J. Am. Chem. Soc. 119 (1997) 9303–9304, https://doi.org/10.1021/ja972171i.
[10] N.N. Mahamuni, Y.G. Adewuyi, Advanced oxidation processes (AOPs) involving ultrasound for waste water treatment: A review with emphasis on cost estimation, Ultrason. Sonochem. 17 (2010) 990–1003, https://doi.org/10.1016/j.ultsonch.2009.09.005.
[11] Y.G. Adewuyi, Sonochemistry in environmental remediation. 1. Heterogeneous sonophotocatalytic oxidation processes for the treatment of pollutants in water, Environ. Sci. Technol. 39 (2005) 3409–3420, https://doi.org/10.1021/es049138y.
[12] Y.G. Adewuyi, Sonochemistry in environmental remediation. 2. Heterogeneous sonophotocatalytic oxidation processes for the treatment of pollutants in water, Environ. Sci. Technol. 39 (2005) 8557–8570, https://doi.org/10.1021/es0509127.
[13] N.H. Ince, Ultrasound-assisted advanced oxidation processes for water decontamination, Ultrason. Sonochem. 40 (2018) 97–103, https://doi.org/10.1016/j.ultsonch.2017.04.009.
[14] Y.G. Adewuyi, Sonochemistry: Environmental science and engineering applications, Ind. Eng. Chem. Res. 40 (2001) 4681–4715, https://doi.org/10.1021/ie010096l.
[15] S. Merouani, H. Ferkous, O. Hamdaoui, Y. Rezgui, M. Guemini, A method for predicting the number of active bubbles in sonochemical reactors, Ultrason. Sonochem. 22 (2015) 51–58, https://doi.org/10.1016/j.ultsonch.2014.07.015.
[16] S. Merouani, O. Hamdaoui, Y. Rezgui, M. Guemini, Sensitivity of free radicals production in acoustically driven bubble to the ultrasonic frequency and nature of dissolved gases, Ultrason. Sonochem. 22 (2015) 41–50, https://doi.org/10.1016/j.ultsonch.2014.07.011.
[17] M. Gągol, A. Przyjazny, G. Boczkaj, Wastewater treatment by means of advanced oxidation processes based on cavitation – A review, Chem. Eng. J. 338 (2018) 599–627, https://doi.org/10.1016/j.cej.2018.01.049.
[18] J. González-García, V. Sáez, I. Tudela, M.I. Díez-Garcia, M. Deseada Esclapez, O. Louisnard, Sonochemical treatment of water polluted by chlorinated organocompounds. A review, Water 2 (2010) 28–74, https://doi.org/10.3390/w2010028.
[19] Q. Hong, J.L. Hardcastle, R.A.J. McKeown, F. Marken, R.G. Compton, The 20 kHz sonochemical degradation of trace cyanide and dye stuffs in aqueous media, New J. Chem. 23 (1999) 845–849, https://doi.org/10.1039/a903990b.
[20] R.H. Jawale, P.R. Gogate, A.B. Pandit, Treatment of cyanide containing wastewater using cavitation based approach, Ultrason. Sonochem. 21 (2014) 1392–1399, https://doi.org/10.1016/j.ultsonch.2014.01.025.
[21] R.H. Jawale, A. Tandale, P.R. Gogate, Novel approaches based on ultrasound for treatment of wastewater containing potassium ferrocyanide, Ultrason. Sonochem. 38 (2017) 402–409, https://doi.org/10.1016/j.ultsonch.2017.03.032.
[22] Z. Bonyadi, A.A. Dehghan, A. Sadeghi, Determination of sonochemical technology efficiency for cyanide removal from aqueous solutions, World Appl. Sci. J. 18 (2012) 425–429, https://doi.org/10.5829/idosi.wasj.2012.18.03.1828.
[23] R.R. Dash, A. Gaur, C. Balomajumder, Cyanide in industrial wastewaters and its removal: A review on biotreatment, J. Hazard. Mater. 163 (2009) 1–11, https://doi.org/10.1016/j.jhazmat.2008.06.051.
[24] M. Shirom, G. Stein, Excited State Chemistry of the Ferrocyanide Ion in Aqueous Solution. I. Formation of the Hydrated Electron, J. Chem. Phys. 55 (1971) 3372–3378.
[25] M.S. Matheson, W.A. Mulac, J. Rabani, Formation of the Hydrated Electron in the Flash Photolysis of Aqueous Solutions 1, J. Phys. Chem. 67 (1963) 2613–2617, https://doi.org/10.1021/j100806a027.
[26] S. Ohno, G. Tsuchihashi, The Photochemistry of Hexacyanoferrate(II) Ions in Aqueous Solutions, Bull. Chem. Soc. Jpn. 38 (1965) 1052–1053.
[27] S. Pommeret, R. Naskrecki, P. Van Der Meulen, M. Ménard, G. Vigneron,

T. Gustavsson, Ultrafast events in the electron photodetachment from the hexacyanoferrate(II) complex in solution, Chem. Phys. Lett. 288 (1998) 833–840, https://doi.org/10.1016/S0009-2614(98)00371-6.
[28] S. Ašpergěr, Kinetics of the decomposition of potassium ferrocyanide in ultra-violet light, Trans. Faraday Soc. 48 (1952) 617–624, https://doi.org/10.1039/TF9524800617.
[29] M. Shirom, G. Stein, Excited State Chemistry of the Ferrocyanide Ion in Aqueous Solution. II. Photoaquation, J. Chem. Phys. 55 (1971) 3379–3382, https://doi.org/10.1016/j.meegid.2009.11.004.
[30] M. Reinhard, T.J. Penfold, F.A. Lima, J. Rittmann, M.H. Rittmann-Frank, R. Abela, I. Tavernelli, U. Rothlisberger, C.J. Milne, M. Chergui, Photooxidation and photoaquation of iron hexacyanide in aqueous solution: A picosecond X-ray absorption study, Struct. Dyn. 1 (2014) 1–12, https://doi.org/10.1063/1.4871751.
[31] M. Reinhard, G. Auböck, N.A. Besley, I.P. Clark, G.M. Greetham, M.W.D. Hanson-Heine, R. Horvath, T.S. Murphy, T.J. Penfold, M. Towrie, M.W. George, M. Chergui, Photoaquation Mechanism of Hexacyanoferrate(II) Ions: Ultrafast 2D UV and Transient Visible and IR Spectroscopies, J. Am. Chem. Soc. 139 (2017) 7335–7347, https://doi.org/10.1021/jacs.7b02769.
[32] S. Merouani, H. Ferkous, O. Hamdaoui, Y. Rezgui, M. Guemini, New interpretation of the effects of argon-saturating gas toward sonochemical reactions, Ultrason. Sonochem. 23 (2015) 37–45, https://doi.org/10.1016/j.ultsonch.2014.09.009.
[33] M.C. Ziskin, P.A. Lewin, Ultrasonic Exposimetry, CRC Press, Boca Raton, 1992.
[34] M. Shirom, G. Stein, The absorption spectrum of the ferrocyanide ion in aqueous solution, Isr. J. Chem. 7 (1969) 405–412.
[35] C.S. Naiman, Interpretation of the Absorption Spectra of K3Fe(CN)6, J. Chem. Phys. 35 (1961) 323–328, https://doi.org/10.1063/1.1731909.
[36] J. Mack, J.R. Bolton, Photochemistry of nitrite and nitrate in aqueous solution : a review, J. Photochem. Photobiol. A Chem. 128 (1999) 1–13.
[37] V. Mišík, P. Riesz, Nitric oxide formation by ultrasound in aqueous solutions, J. Phys. Chem. 100 (1996) 17986–17994, https://doi.org/10.1021/jp961522x.
[38] E.L. Mead, R.G. Sutherland, R.E. Verrall, The effect of ultrasound on water in the presence of dissolved gases, Can. J. Chem. 54 (1976) 1114–1120, https://doi.org/10.1139/v76-159.
[39] P. Supeno, Kruus, Sonochemical formation of nitrate and nitrite in water, Ultrason. Sonochem. 7 (2000) 109–113, https://doi.org/10.1016/S1350-4177(99)00043-7.
[40] J. Yao, L. Chen, X. Chen, L. Zhou, W. Liu, Z. Zhang, Formation of inorganic nitrogenous byproducts in aqueous solution under ultrasound irradiation, Ultrason. Sonochem. 42 (2018) 42–47, https://doi.org/10.1016/j.ultsonch.2017.10.033.
[41] G.V. Buxton, C.L. Greenstock, W.P. Helman, A.B. Ross, Critical Review of Rate Constants for Reactions of Hydrated Electrons, Hydrogen Atoms and Hydroxyl Radicals (· OH /· O-) in Aqueous Solution, J. Phys. Chem. Ref. Data. 17 (1988) 513–886, https://doi.org/10.1063/1.555805.
[42] A. Khlyustova, N. Khomyakova, N. Sirotkin, Y. Marfin, The Effect of pH on OH Radical Generation in Aqueous Solutions by Atmospheric Pressure Glow Discharge, Plasma Chem. Plasma Process. 36 (2016) 1229–1238, https://doi.org/10.1007/s11090-016-9732-3.
[43] S. Rajendran, R.J. Rathish, S.S. Prabha, A. Anandan, Green electrochemistry – a versatile tool in green synthesis: an overview, Port. Electrochim. Acta 34 (2016) 321–342, https://doi.org/10.4152/pea.201605321.
[44] D. Zehavi, J. Rabani, Pulse Radiolysis of the Aqueous Ferro-Ferricyanide System. II. Reactions of Hydrogen Atoms and eaq- with Ferrocyanide and Ferricyanide Ions, J. Phys. Chem. 78 1368–1373 (1974), https://doi.org/10.1021/j100607a006.
[45] V. Misik, P. Riesz, Evidence against the formation of hydrated electrons as principal species in the sonochemistry of neutral aqueous solutions, Proc. Annu. Meet. Japan Soc. Sonochem. 6 (1997) 5–8.
[46] L. Dharmarathne, M. Ashokkumar, F. Grieser, On the generation of the hydrated electron during the sonolysis of aqueous solutions, J. Phys. Chem. A 117 (2013) 2409–2414, https://doi.org/10.1021/jp312389n.
[47] S. Golbaz, A.J. Jafari, R.R. Kalantari, The study of Fenton oxidation process efficiency in the simultaneous removal of phenol, cyanide, and chromium (VI) from synthetic wastewater, Desalin. Water Treat. 51 (2013) 5761–5767, https://doi.org/10.1080/19443994.2012.760108.
[48] S.I. Nikitenko, R. Pflieger, Toward a new paradigm for sonochemistry: Short review on nonequilibrium plasma observations by means of MBSL spectroscopy in aqueous solutions, Ultrason. Sonochem. 35 (2015) 623–630, https://doi.org/10.1016/j.ultsonch.2016.02.003.
[49] T. Thanh Nguyen, Y. Asakura, S. Koda, K. Yasuda, Dependence of cavitation, chemical effect, and mechanical effect thresholds on ultrasonic frequency, Ultrason. Sonochem. 39 (2017) 301–306, https://doi.org/10.1016/j.ultsonch.2017.04.037.
[50] B.N. Aronstein, R.A. Lawal, A. Maka, Chemical degradation of cyanides by fenton's reagent in aqueous and soil-containing systems, Environ. Toxicol. Chem. 13 (1994) 1719–1726, https://doi.org/10.1002/etc.5620131102.
[51] G.L. Sharipov, A.M. Abdrakhmanov, B.M. Gareev, L.R. Yakshembetova, Sonochemiluminescence in an aqueous solution of Ru(bpy)3Cl2, Ultrason. Sonochem. 42 (2018) 526–531, https://doi.org/10.1016/j.ultsonch.2017.12.013.
[52] I. Hua, M.R. Hoffmann, Optimization of ultrasonic irradiation as an advanced oxidation technology, Environ. Sci. Technol. 31 (1997) 2237–2243, https://doi.org/10.1021/es960717f.
[53] J. Rooze, E.V. Rebrov, J.C. Schouten, J.T.F. Keurentjes, Effect of resonance frequency, power input, and saturation gas type on the oxidation efficiency of an ultrasound horn, Ultrason. Sonochem. 18 (2011) 209–215, https://doi.org/10.1016/j.ultsonch.2010.05.007.
[54] J.D. Seymour, H.C. Wallace, R.B. Gupta, Sonochemical reactions at 640 kHz using an efficient reactor. Oxidation of potassium iodide, Ultrason. Sonochem. 4 (1997) 289–293.